DOI: 10.1002/cmdc.200700181

A Study of the Binding Energies of Efavirenz to Wild-Type and K103N/Y181C HIV-1 Reverse Transcriptase Based on the ONIOM Method

Pensri Srivab[a] and Supa Hannongbua*[a, b]

A three-layered ONIOM model was used to study the interactions between efavirenz and the binding sites of HIV-1 reverse transcriptase (RT): wild-type and double mutant K103N/Y181C enzyme forms. Binding energies were determined and compared to describe the loss of activity of efavirenz with the mutant HIV-1 RT binding pocket. The calculated binding energy for the efavirenz–K103N/Y181C HIV-1 RT complex is less than that with the wild-type complex by approximately 8 kcal mol^{-1}. The interaction energies, calculated at the MP2/6-31G(d,p) level between efavirenz and individual residues surrounding the binding pocket of the K103N/Y181C enzyme, demonstrate that the attractive interactions between efavirenz and residue positions 101 and 103 were less than those for wild-type RT by 5.52 and 3.62 kcal mol^{-1}, respectively. Understanding these interactions could be useful in the design of inhibitors specific for the HIV-1 RT allosteric site and that have greater potency against the mutant enzyme.

Introduction

Human immunodeficiency virus type 1 reverse transcriptase (HIV-1 RT) is an attractive target for the development of new anti-AIDS drugs. It is an asymmetric heterodimer consisting of p66 and p51 subunits, and plays an important role for virus replication from a single-stranded viral RNA into a double-stranded DNA prior to integration into the genome of the human host cell.[1] The inhibitors of HIV-1 RT can be divided into two main classes: nucleoside reverse transcriptase inhibitors (NRTIs) and non-nucleoside reverse transcriptase inhibitors (NNRTIs).[2] NRTIs inhibit HIV replication by terminating DNA chain elongation. Many of these drugs are competitive inhibitors, which have high cellular toxicity and produce several side effects. In the case of noncompetitive inhibitors, NNRTIs are highly specific directly bound to HIV-1 RT at an allosteric site which is removed from the polymerase active site by approximately 10 Å. Binding of NNRTIs to the allosteric site, distorts the three-dimensional active site of HIV-1 RT causing loss of catalytic function.[3]

Although NNRTIs are highly specific and much less toxic than NRTIs, their therapeutic effectiveness is limited by the rapid emergence of HIV-1 mutations that are often resistant to current drugs.[4] In this study, K103N/Y181C HIV-1RT complexed with efavirenz was chosen to investigate the binding energy. Efavirenz bound to the wild-type and mutated HIV-1 RTs such as the K103N or the Y181C enzymes has been extensively studied in both experimental and computational methods. X-ray crystallographic structures of efavirenz in complexes with wild-type and single mutant type (K103N or Y181C) HIV-1 RT were determined. These results led to an understanding of some structural factors that confer resilience to drug-resistance mutation.[5] Efavirenz shows about a 6.0, 2.5 and ninefold decrease in binding to K103N, Y181C and K103N/Y181C HIV-1 RT, respectively, relative to wild-type HIV-1 RT.[6]

Recently, the efavirenz-HIV-1 RT interaction was studied using computational chemistry. Monte Carlo extended linear response (MC/ELR) calculations were used to predict the activity of efavirenz analogues with the single mutation of HIV-1 RT and identify factors controlling binding with K103N HIV-1 RT.[7] In order to understand the effect of the K103N mutation of HIV-1 RT on the activity of efavirenz analogues, Monte Carlo/free energy perturbation (MC/FEP) calculations were applied.[8] A series of targeted molecular dynamics (MD) simulations were studied on the effect of K103N HIV-1 RT on the binding of NNRTI, including efavirenz.[9] Moreover, Molecular Mechanics Poisson–Boltzmann/surface area (MM-PBSA) combined with molecular docking calculations were used to calculate binding energy and predict the potential binding mode of efavirenz derivatives in the HIV-1 RT binding pockets.[10] Then, docking calculations were subjected to 3D QSAR studies using CoMFA and CoMSIA to obtain the binding conformation and the structure–activity correlation of HIV-1 RT inhibitors of efavirenz and wild-type and K103N HIV-1 RT.[11] However, the HIV-1 RT/efavirenz complex structure is difficult to model using ab initio quantum chemical calculations owing to its size and complexity. Other methods have been developed to study large molecular systems including quantum mechanics/molecular mechanics (QM/MM),[12] molecular fractionation with conjugate caps (MFCC),[13] and our own n-layered integrated molecular orbital and molecular mechanics (ONIOM).[14]

[a] *P. Srivab, Prof. Dr. S. Hannongbua*
Department of Chemistry, Faculty of Science
Kasetsart University, Bangkok 10900 (Thailand)
Fax: (+66) 2-5625555 ext. 2140
E-mail: fscisph@ku.ac.th

[b] *Prof. Dr. S. Hannongbua*
Center of Nanotechnology and NANOTEC Center of Excellence
Kasetsart University, Bangkok 10900 (Thailand)

MFCC was developed by Zhang and co-workers and was used to study binding of efavirenz to HIV-1 RT for both wild-type and single mutant types such as Y181C or K103N enzymes.[13] It was found that the small loss of binding to the K103N mutant by efavirenz can be attributed to a slightly weakened attractive interaction between the drug and K101 residue. The small loss of binding to the Y181C mutation by efavirenz can be attributed to the Glu138(b) residue from the 51 domain of RT moving closer to efavirenz, which results in an increase of repulsive energy relative to the wild-type. The ONIOM method[15] has recently been used as a powerful hybrid method to study biological systems. The actual reaction in biological systems occur only in a small region known as the active center, which is treated with the highest level ab initio QM method, while outer layers are treated with less computationally expensive QM methods, such as low level QM, semiempirical or MM methods. Recently, the ONIOM method was successfully used to calculate the interaction energies and the binding energies of TIBO and nevirapine in the HIV-1 RT binding pocket. These results reveal the effects of surrounding residues on the NNRTI.[16] The two-layer ONIOM (ONIOM2) method was performed to study the interaction between efavirenz and residues in the binding pocket for wild-type HIV-1 RT.[17] The results showed a net attractive interaction between efavirenz and surrounding residues, and K101 residue demonstrated a stronger interaction than others; this interaction plays an important role in the stability of the inhibitor and strengthens the inhibitory affinity of efavirenz over other NNRTIs.

In an attempt to understand the different binding stabilities of efavirenz to wild-type and double mutant HIV-1 RT at a molecular level, the ONIOM computational approach was employed. This approach was useful in previous studies to demonstrate the particular interaction between the NNRTIs and amino acids in the non-nucleoside inhibitor binding pocket (NNIBP) with wild-type and single mutant HIV-1 RT. In particular, the weaker inhibitory effect of efavirenz to the double mutant strain has not been clearly understood. The following work describes how the binding interaction of efavirenz to the double mutant K103N/Y181C HIV-1 RT is important and results in the loss of binding stability with the mutant enzyme. It is expected that this understanding will be helpful in the design of new inhibitors especially active against double mutant HIV-1 RT, and thus better anti-AIDS agents.

Computational Methods

Systems studied

The starting models for calculations were obtained from the X-ray structures of efavirenz bound to the wild-type RT, listed in the Protein Data Bank with PDB entry code 1FK9.[5b] In this study, K103N/Y181C HIV-1 RT was modeled from PDB entry code 1IKV[5b] by replacing Y181 with C181 as there is no crystallographic structure available. The studied binding pocket included residues surrounding the NNIBP with at least one atom interacting with any of the atoms of efavirenz within an interatomic distance of 7.0 Å. These residues include Pro95, Leu100, Lys101, Lys102, Lys103(Asn103), Lys104, Ser105, Val106, Val179, Ile180, Tyr181(Cys181), Tyr188, Val189, Gly190, Phe227, Leu228, Trp229, Leu234, His235, Pro236 and Tyr318 from the p66 domain of RT, and Glu138(b) from the 51 domain of RT (Figure 1). All residues were assumed to be in their neutral

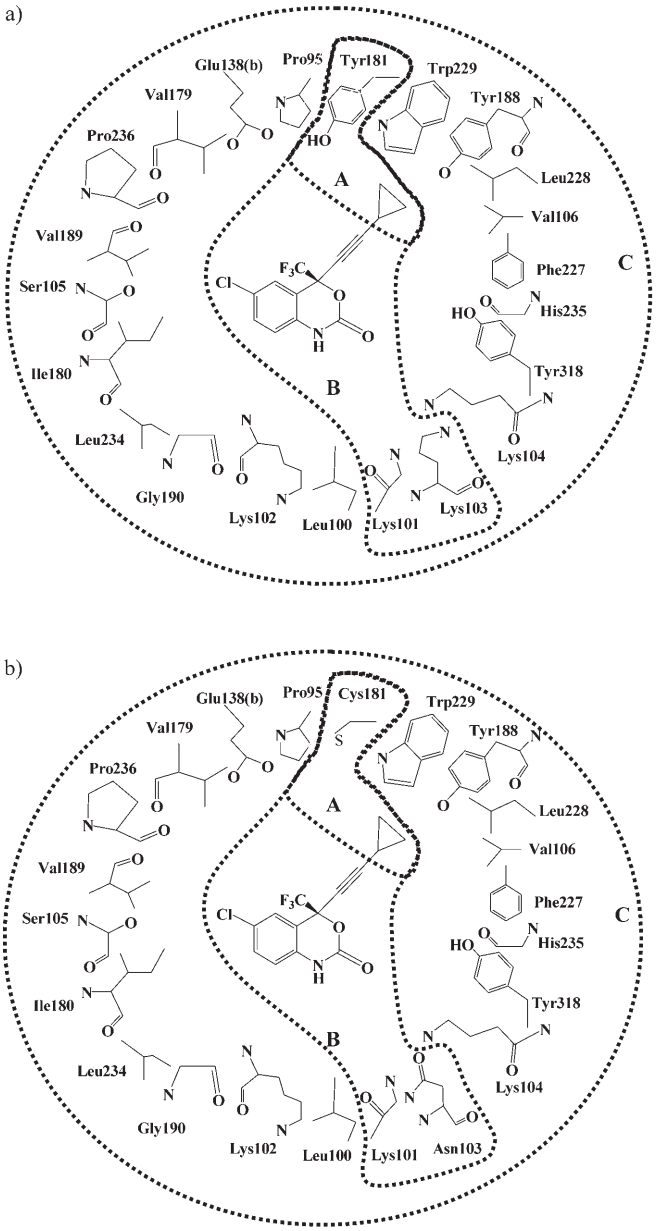

Figure 1. Model system consisting of 22 residues used for efavirenz bound to allosteric sites of HIV-1 RT: a) wild-type HIV-1 RT NNIBP and b) K103N/Y181C HIV-1 RT NNIBP.

form. The N- and C-terminal ends of cut residues were capped with an acetyl group (CH_3CO-) and methyl amino group (-$NHCH_3$), respectively [(H_3C-C(=O)-{NH-CH(-R)-C(=O)}$_n$-NH-CH_3)]. Hydrogen atoms were then added to generate the complete structures and their positions were optimized by the semiempirical PM3 method as available in the GAUSSIAN 03

program[18] running in Linux on a Pentium IV 3.2 GHz PC. The optimizations were carried out with fixed heavy atoms and the final structures produced were used as the starting geometries for all subsequent calculations.

Interaction energy calculations

The interaction energies ($E_{(EFZ+Xi)}$) between efavirenz (EFZ) and individual residues (X_i) were calculated as a single point calculation at the B3LYP/6-31G(d,p) and MP2/6-31G(d,p) levels of calculations using the geometry described above. The total interaction energy (INT) can be expressed as:[16a]

$$INT_{(EFZ+Xi)} = E_{(EFZ+Xi)} - E_{(EFZ)} - E_{(Xi)} \quad (1)$$

in which $E_{(EFZ)}$ and $E_{(Xi)}$ are energies of efavirenz and each individual residue, respectively.

Binding energy calculations

The binding energy (BE) of efavirenz bound to the allosteric pocket of the K103N/Y181C HIV-1 RT, relative to the wild-type, was determined using Equation (2) and followed details for the three-layered ONIOM (ONIOM3) methods.[16b] All calculations were carried out using the GAUSSIAN 03 package:[18]

$$\begin{aligned} BE^{ONIOM3} &= E[Cpx]_{opt} - E[P]_{opt} - E[L]_{opt} \\ &= \Delta E\ (\text{High, A}) + [\Delta E\ (\text{Mid, AB}) - \Delta E\ (\text{Mid, A})] \\ &\quad + [\Delta E\ (\text{Low, ABC}) - \Delta E\ (\text{Low, AB})] \\ &= \Delta E\ (\text{High, A}) + [\Delta\Delta E\ (\text{Mid, AB-A})] \\ &\quad + [\Delta\Delta E\ (\text{Low, ABC-AB})] \end{aligned} \quad (2)$$

for which $E[Cpx]_{opt}$ is the total optimized energy of the efavirenz–binding pocket complex (Cpx), $E[P]_{opt}$ is the optimized energy of the binding pocket, and $E[L]_{opt}$ is the optimized energy of the efavirenz ligand. Also, ΔE (High, A) is the interaction energy in region A which is treated at the highest level of calculations; $\Delta\Delta E$ (Mid, AB-A) is the interaction energy from interactions between the regions A and B and is evaluated at the medium level of calculations; $\Delta\Delta E$ (Low, ABC-AB) is the interaction energy from interactions between regions AB and C which is evaluated at the low level of calculations.

In the inner layer, the cyclopropylethynyl side chain of efavirenz interacts with the aromatic side chain of Y181. Therefore, MP2 calculations were used in order to take into account the H–π interaction.[16b] Thus, the inner layer (Figure 1, region A) was treated at the MP2/6-31G(d,p) level of theory. The medium layer (Figure 1, region B), including the remainder of the efavirenz structure, K101, and K103 (or N103) residues, was treated at the HF/6-31G(d,p) and B3LYP/6-31G(d,p) levels of theory. The outer layer (Figure 1, region C) was treated by the semi-empirical PM3 method. Based on these partition systems, the two types of ONIOM3 methods, MP2/6-31G(d,p):HF/6-31G(d,p):PM3 and MP2/6-31G(d,p):B3LYP/6-31G(d,p):PM3, were analyzed.

Table 1. Calculated interaction energies of efavirenz with individual residues (X_i) from B3LYP/6-31G(d,p) and MP2/6-31G(d,p) methods.

Residue	B3LYP/6-31G(d,p)			MP2/6-31G(d,p)		
	Wild-type	K103N/Y181C	ΔE^a	Wild-type	K103N/Y181C	ΔE^b
P95	−0.33	−0.35	0.02	−1.09	−1.09	0.00
L100	−0.56	0.16	−0.71	−7.66	−6.11	−1.54
K101	−12.49	−8.08	−4.41	−14.81	−9.29	−5.52
K102	1.01	0.47	0.54	0.17	−0.37	0.54
K103(N)	−1.08	(0.42)	−1.50	−5.15	(−1.53)	−3.62
K104	0.11	−0.16	0.27	0.04	−0.29	0.33
S105	0.06	0.35	−0.28	−0.06	0.22	−0.28
V106	1.08	0.71	0.37	−2.59	−3.76	1.17
V179	1.61	−1.80	3.41	0.06	−3.60	3.67
I180	−0.17	−0.17	0.00	−0.50	−0.40	−0.11
Y181(C)	−0.25	(−1.17)	0.92	−3.87	(−3.32)	−0.55
Y188	−1.14	−0.52	−0.62	−6.21	−5.54	−0.68
V189	−0.49	−0.52	0.02	−1.09	−1.17	0.08
G190	−1.03	−0.83	−0.19	−1.75	−1.45	−0.30
F227	0.07	0.28	−0.21	−1.04	−1.59	0.55
L228	−0.06	0.02	−0.08	−0.08	−0.02	−0.06
W229	−0.86	1.44	−2.30	−3.24	−4.07	0.83
L234	0.15	2.95	−2.80	−1.96	−0.31	−1.66
H235	−1.58	−0.78	−0.79	−2.87	−2.32	−0.56
P236	−0.55	0.50	−1.06	−2.81	−1.45	−1.36
Y318	−0.37	−0.83	0.46	−2.87	−3.50	0.64
E138(b)	1.83	0.12	1.72	1.26	−0.09	1.35
Total	−15.04	−8.63	−7.22	−58.12	−51.05	−7.07

$\Delta E = E_{\text{wild-type}} - E_{\text{K103N/Y181C}}$.

Results and Discussion

Interaction energy calculations

The interaction energies between efavirenz and the individual residues (X_i) of the HIV-1 RT binding pocket for wild-type and K103N/Y181C enzymes were calculated at the B3LYP/6-31G(d,p) and MP2/6-31G(d,p) levels of theory and are shown in Table 1. As the MP2 method includes the dispersion interactions, it is expected to give more accurate interaction energies than B3LYP.[19] The results show that the MP2 calculations give lower interaction energies than B3LYP results at the same basis set, and the relative interaction energies (ΔE^a and ΔE^b in Table 1) for both B3LYP/6-31G(d,p) and MP2/6-31G(d,p) levels of theory are consistent. In the wild-type, the main contributions to the interactions with efavirenz come from L100, K101, K103, Y181, Y188 and W229 which produce attractive interactions greater than 3 kcal mol^{-1}, calculated at the MP2/6-31G(d,p) level of theory. It was found that benzoxine-2-one (–NH and –C=O) in efavirenz interacts with the backbone carbonyl

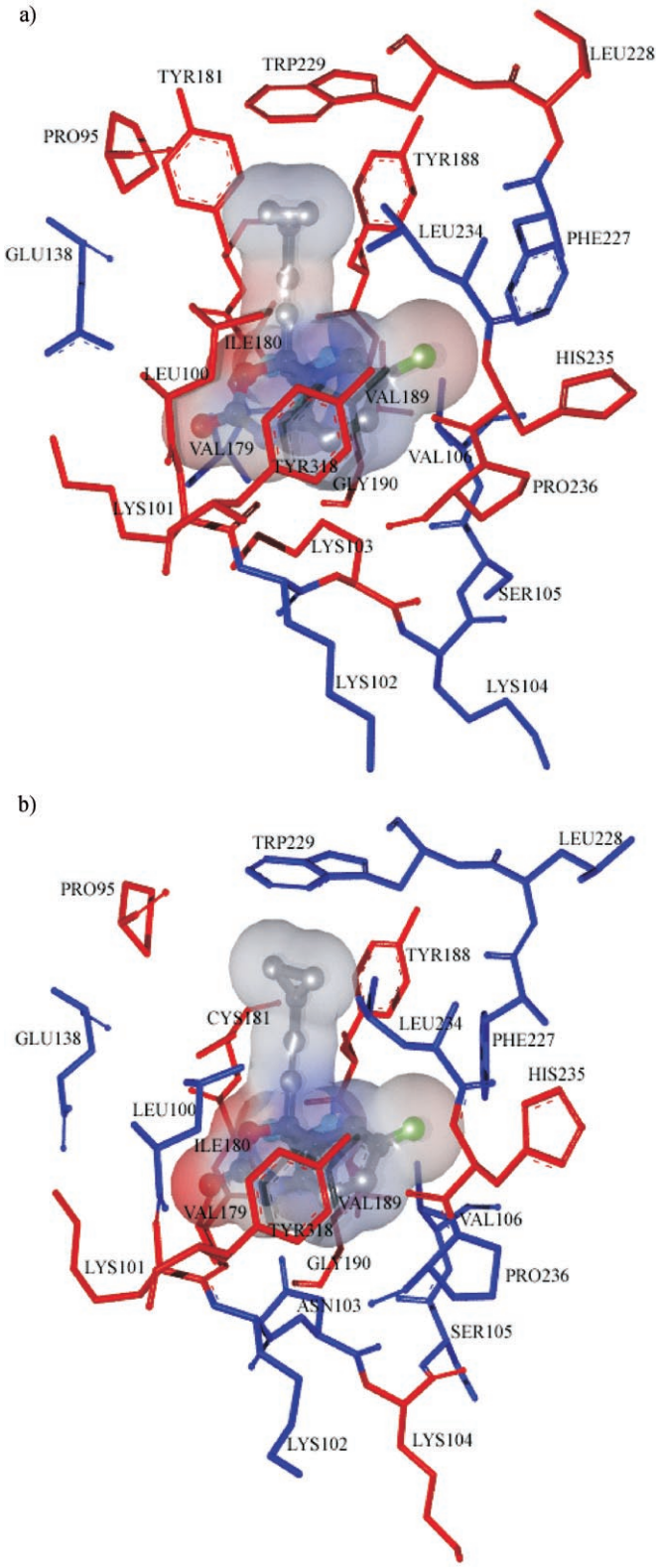

Figure 2. Residues having attractive interactions (red) and repulsive interactions (blue) with efavirenz are shown for a) wild-type and b) K103N/Y181C enzymes.

oxygen (C=O) and amino hydrogen (–NH) of K101, exhibiting moderate hydrogen bonding[17] and causing the strongest interaction: −14.81 kcal mol^{-1}.

Figure 2 shows the residues color-coded according to attractive and repulsive interactions. It can be observed that there are more repulsive interactions between efavirenz and residues of the binding pocket for the K103N/Y181C enzyme (Figure 2b) than the wild-type (Figure 2a). Also, the attractive interactions between efavirenz and K101 and K103 residues in the K103N/Y181C enzyme were decreased to 5.52 and 3.62 kcal mol^{-1} (ΔE^b in Table 1, MP2/6-31G(d,p) calculations), respectively, compared with wild-type RT. In the case of V179, the strong attractive interaction was observed to change from 0.06 to −3.06 kcal mol^{-1}. These results indicate that the mutated residues (K103N/Y181C) not only decrease the binding stability of efavirenz, but also induce destabilization in the cavity leading other residues to lose contact or have drastically changing interactions with the inhibitor.

Binding energy calculations

From Table 1, the double mutation of K103N/Y181C HIV-1 RT leads to the main loss of contact between efavirenz and K101 and N103, which reduce the individual interaction energy by 5.52 and 3.62 kcal mol^{-1}, respectively. Efavirenz interacting with Y181 through the hydrogen atoms of its cyclopropylethynyl group with the aromatic ring of the residue was considered as part of the interacting core for ONIOM3 calculations. For increased accuracy, the MP2 method was used in ONIOM3 calculations to include these dispersion interactions.[16b] Table 2 shows the binding energies with basis set superposition error (BSSE)[20] for the wild-type and K103N/Y181C complexes. It was found that the binding energies from MP2/6-31G(d,p):HF/6-31G(d,p):PM3 and MP2/6-31G(d,p):B3LYP/6-31G(d,p):PM3 methods obtained from both methods of calculations are not significantly different (~1 kcal mol^{-1}). The differences in binding energies between wild-type and K103N/Y181C enzymes are far more significant (7.51 and 7.91 kcal mol^{-1} from MP2/6-31G(d,p):HF/6-31G(d,p):PM3 and MP2/6-31G(d,p):B3LYP/6-31G(d,p):PM3 methods, respectively). Only the interaction energy between region A and B [$\Delta\Delta E$ (Mid, AB-A)] of the K103N/Y181C enzyme (−3.78 kcal mol^{-1}) is less than that in the wild-type (−9.21 kcal mol^{-1}), with the greatest difference of 5.43 kcal mol^{-1}. It causes a large reduction in attractive interactions between efavirenz and residues in region B (K101 and N103). This corresponds to weakened hydrogen bonds between benzoxine-2-one (–NH and –C=O) of efavirenz and the backbone carbonyl oxygen (C=O) and amino hydrogen (-NH) of K101 (Table 3). The hydrogen bonding distances between benzoxine-2-one and K101 from MP2/6-31G(d,p):HF/6-31G(d,p):PM3 and MP2/6-31G(d,p):B3LYP/6-31G(d,p):PM3 calculations corresponded well with the X-ray crystallographic data. Moreover, N103 creates repulsive interactions with efavirenz (Figure 3b) when compared with the interaction between K103 and efavirenz (Figure 3a). The interaction energies between regions AB and C [$\Delta\Delta E$ (Low, ABC-AB)] of the K103N/Y181C enzyme (−5.42 kcal mol^{-1}) are less than the wild-type (−7.04 kcal mol^{-1}) by 1.62 kcal mol^{-1}. This indicates the mutations, K103N/Y181C, induce a slight loss of contact of residues in region C with efavirenz. The interaction energy from MP2/6-

Table 2. Binding energy and components of binding energy with BSSE corrections for wild-type and K103N/Y181C HIV-1 RT complexed with efavirenz by the ONIOM3 method.

ONIOM3 Method	Calculated energies [kcal mol^{-1}]			
	BE	ΔE (High, A)[a]	$\Delta\Delta E$ (Mid, AB-A)	$\Delta\Delta E$ (Low, ABC-AB)
MP2/6-31G(d,p):HF/6-31G(d,p):PM3				
Wild-type	−15.60	−0.67	−8.61	−6.32
K103N/Y181C	−8.09	0.14	−3.50	−4.73
ΔE	−7.51	−0.81	−5.11	−1.59
MP2/6-31G(d,p):B3LYP/6-31G(d,p):PM3				
Wild-type	−16.91	−0.66	−9.21	−7.04
K103N/Y181C	−9.00	0.20	−3.78	−5.42
ΔE	−7.91	−0.86	−5.43	−1.62
Experimental binding loss			ninefold	

[a] $\Delta E = E_{\text{wild-type}} - E_{\text{K103N/Y181C}}$.

Table 3. Calculated heteroatomic hydrogen bond lengths [Å] between benzoxine-2-one (-NH and -C=O) of efavirenz and the backbone carbonyl oxygen (C=O) and amino hydrogen (-NH) atoms of K101, based on the ONIOM3 method for wild-type and K103N/Y181C HIV-1 RT in comparison with X-ray crystallographic data.

ONIOM3 Method	Wild-type		K103N/Y181C[a]	
	-C=O$_K$···H–N$_B$-	-N–H$_K$···O=C$_B$-	-C=O$_K$···H–N$_B$-	-N–H$_K$···O=C$_B$-
MP2/6-31G(d,p):HF/6-31G(d,p):PM3	2.86	3.12	2.92(0.06)	3.54(0.42)
MP2/6-31G(d,p):B3LYP/6-31G(d,p):PM3	2.80	3.03	2.85(0.05)	3.46(0.43)
X-ray crystal data	2.75	3.17	3.01(0.26)	3.61(0.44)

[a] Values in parentheses represent the lengthening hydrogen bonding in the double mutant complex relative to the wild-type complex.

31G(d,p):B3LYP/6-31G(d,p):PM3 calculations in region A, between the cyclopropylethynyl group and Y181, is weakly attractive for the wild-type (−0.66 kcal mol^{-1}) and weakly repulsive for C181 (0.20 kcal mol^{-1}). This can be explained by the fact that the mutation, Y181C, causes a loss of contact between efavirenz and C181 leading to a weakly repulsive interaction in region A (0.20 kcal mol^{-1}). The calculated binding energy of the K103N/Y181C complex is less than that of the wild-type complex by 7.91 kcal mol^{-1}, which agrees well with the experimentally observed ninefold decrease in binding. Notably, the mutations in the K103N/Y181C enzyme eliminate favorable contacts of the aromatic ring of the Y181 and hydrocarbon side chain of K103 with efavirenz. This leads to a decrease in the stabilization energy of the complex and induces destabilization in the cavity by reducing contact between the main contributor (K101) and mutated residues (N103 and C181) with efavirenz. This is consistent with the observation that efavirenz shows higher inhibitory affinities with the wild-type than the double mutation K103N/Y181C enzyme.

Comparison of the modeled complex structure with the double mutant complex structure

Recently, only a crystal structure (PDB code: 2IC3) of K103N/Y181C HIV-1 RT complex with HBY097 (Figure 4) was available.[21] Therefore, we compared the modeled structure used in this work and the X-ray structure of the double mutant enzyme. Superposition of the modeled structure of the K103N/Y181C HIV-1 RT complex and efavirenz and the X-ray structure of K103N/Y181C HIV-1 RT/HBY097 was performed and the result is shown in Figure 5. RMSD (root mean squares deviation) between the whole system of the modeled structure and the X-ray structure is 1.22 Å. Comparison between the binding pocket of the modeled structure and the X-ray structure, gives an RMSD of 0.97 Å. These results confirmed that the modeled structure and X-ray structure of the double mutant enzyme are not significantly different.

Next, efavirenz was superimposed on the HBY097 inhibitor in the binding pocket of K103N/Y181C HIV-1 RT obtained from X-ray crystallographic structure. Then, this structure was used as the starting geometry for binding energy calculations for efavirenz bound to K103N/Y181C HIV-1 RT obtained from the X-ray structure and the results were compared with those obtained from the modeled complex structure. We tested the system with the ONIOM2 method because the calculated binding energies from ONIOM2 and ONIOM3 are not significantly different.[16] Consequently, the binding energies of efavirenz bound to K103N/Y181C HIV-1 RT obtained from the modeled structure and X-ray structure are −6.82 and −8.04 kcal mol^{-1}, respectively. By using ONIOM2 (B3LYP/6-31G(d,p):PM3) method, the difference of the binding energy is found to be 1.22 kcal mol^{-1}. This indicates that the modeled structure of the double mutant enzyme in this study can be used to represent the structure of K103N/Y181C HIV-1 RT.

Comparison of different binding modes of efavirenz and some other NNRTIs

Drug resistance mutation is the key problem which must be addressed to develop better inhibitors. Thus, the understanding of the molecular mechanism of drug resistance can help in the design of better inhibitors. Here, we discuss the drug resistance of efavirenz as compared with the less potent inhibitor (nevirapine) and the more potent diarylpyrimidine (DAPY) NNRTIs in molecular details. K103N and Y181C mutation are the most frequently observed mutations in the patients treated with NNRTIs. Efavirenz fails to treat the K103N mutation. The Y181C mutation, confers resistance to nevirapine. The combined two mutations, K103N and Y181C, are resistant to almost all NNRTIs drugs including nevirapine and efavirenz. However, the diarylpyrimidine (DAPY) NNRTIs, including

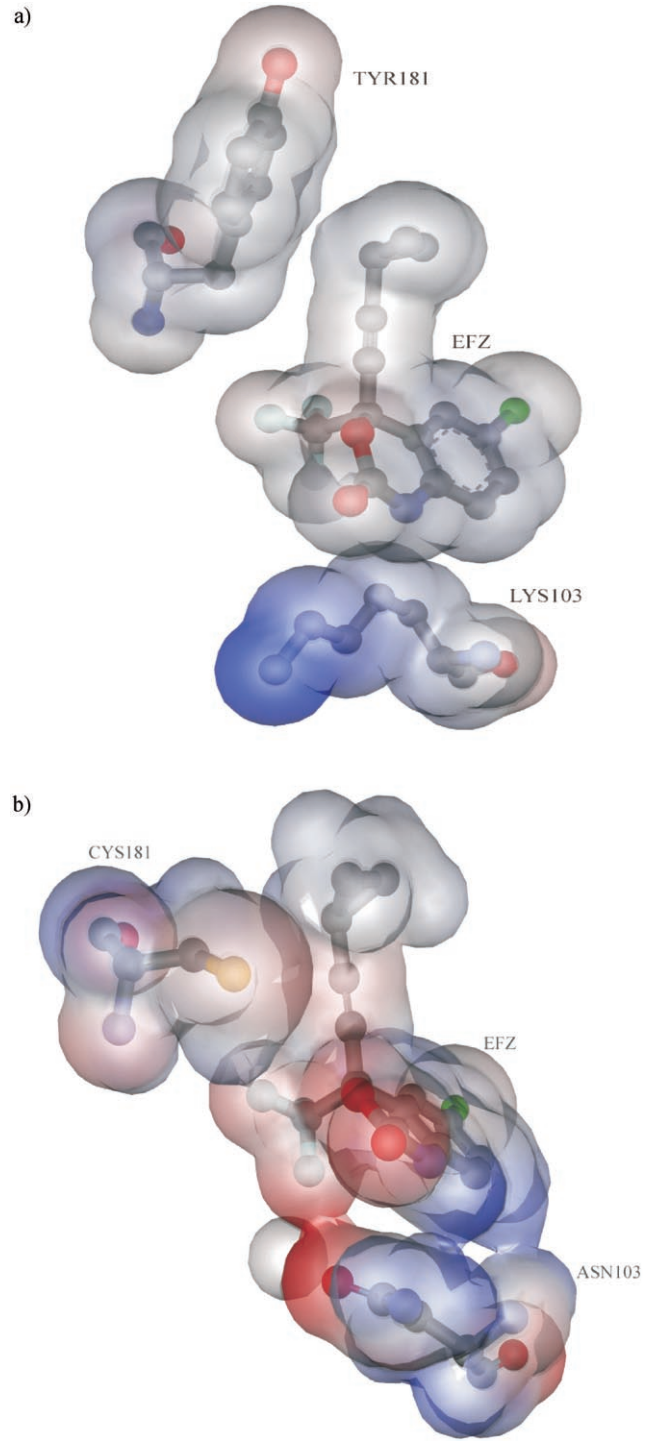

Figure 3. Electrostatic potential is shown on the van der Waals accessible surface, with red for negative and blue for positive values: a) efavirenz interacting with Y181 and K103 in wild-type RT and b) efavirenz interacting with C181 and N103 in the K103N/Y181C mutant form.

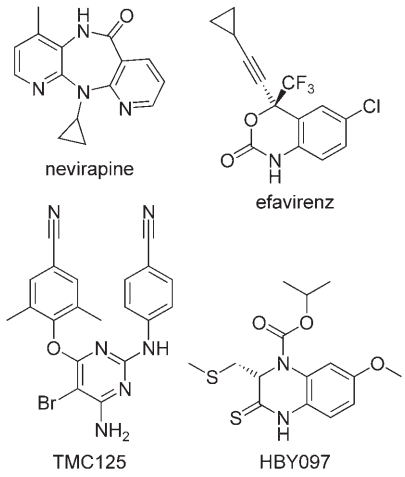

Figure 4. Chemical structures of nevirapine, efavirenz, TMC125 and HBY097.

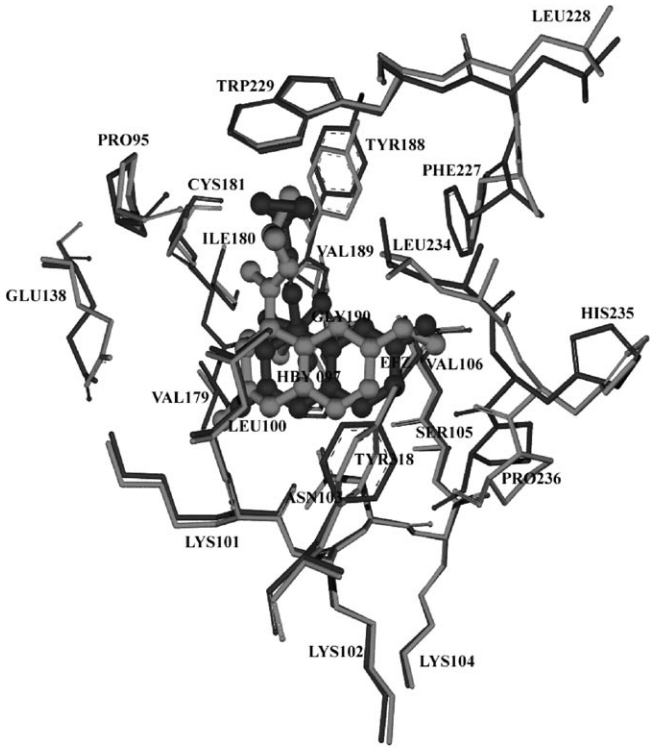

Figure 5. Superposition between the modeled structure of K103N/Y181C HIV-1 RT in complex with efavirenz (dark gray) and in complex with HBY097 (light gray) obtained from the X-ray crystallographic structure.

TMC125 (etravirine), TMC278 (rilpivirine) and analogues of TMC278 effectively inhibit K103N/Y181C HIV-1 RT.[22]

The structural complex of K103N/Y181C HIV-1 RT/NNRTIs was prepared by a docking method. NNRTIs including efavirenz, nevirapine and TMC125 (Figure 4) were docked into the binding pocket of K103N/Y181C HIV-1 RT (PDB code: 2IC3) using Autodock 3.05.[23] A crystal structure of K103N/Y181C HIV-1 RT with HBY097 is available, but there is no crystal structure of K103N/Y181C HIV-1 RT complex with these three inhibitors, therefore, the structures of the double mutant enzyme complex with efavirenz, nevirapine and TMC125 (Figure 5) were prepared by Autodock 3.05. [23] First, the HBY097 compound was docked back into the K103N/Y181C HIV-1 RT binding pocket with an RMSD value of 0.52 Å. This result indicated that the binding mode of the docked HBY097 shows similar in-

teraction with the X-ray crystallographic structure. Therefore, ten independent docking runs were carried out for each ligand. Docked conformations representing the lowest final docked energy were then selected. The docking results indicated that these three inhibitors bind in the same site of K103N/Y181C HIV-1 RT as shown in Figure 6 and 7.

Consequently, the binding of efavirenz and nevirapine with K103N/Y181C HIV-1 RT were compared. Nevirapine as a first-generation NNRTI is effective against wild-type HIV-1 RT, but it has significantly lower potency when tested against mutant enzymes. Its structure contains aromatic rings that have π–π interactions with aromatic amino acids (Y181, Y188, P227, W229, and Y318) in a binding pocket of HIV-1 RT. The Y181C mutation decreases favorable π–π interactions between the aromatic side chain of tyrosine 181 and nevirapine, leading to high levels of resistance to nevirapine. For the K103N mutation, nevirapine is stabilized by the formation of a hydrogen bond between the N103 side chain and the Y188 phenoxy oxygen.[24] The structure of nevirapine is rigid. Efavirenz can adapt itself within the pocket and shows a small loss activity to the mutations. Several structural features of efavirenz are in common with nevirapine (Figure 6). The trifluoromethyl group of efavirenz occupies the same space as the cyclopropyl group of nevirapine. In addition, the cyclopropylethynyl group of efavirenz, which is surrounded by the aromatic side chains of Y181, Y188, W229, and F227, overlaps with the pyridine ring of nevirapine. This limits the interaction of efavirenz and side chains of Y181 and Y188. Whenever the aromatic side chain of Y181 changes to a smaller non-aromatic side chain such as cysteine, this has less effect on the binding of efavirenz to the Y181C mutation. The other feature of the benzoxine-2-one ring of efavirenz binding to HIV-1 RT include sandwiching between the side chains of L100 and V106, and hydrogen bonding with the backbone carbonyl oxygen (C=O) and amino hydrogen (–NH) of K101.[17] This phenomenon is not present in the case of nevirapine (Figure 6 b). With Y181C or K103N HIV-1 RT mutations the hydrogen bond between efavirenz and K101 still remains and acts as the strongest interaction. On the other hand, the N103 mutated position in K103N/Y181C HIV-1 RT disturbs only one hydrogen bond distance between –C=O of the benzoxine-2-one ring of efavirenz and the backbone amino hydrogen (-NH) of K101. This causes a large reduction in attractive interactions between efavirenz and the K101 residue in the K103N/Y181C HIV-1 RT mutation. These structural observations help to develop new potent inhibitors for the mutations.

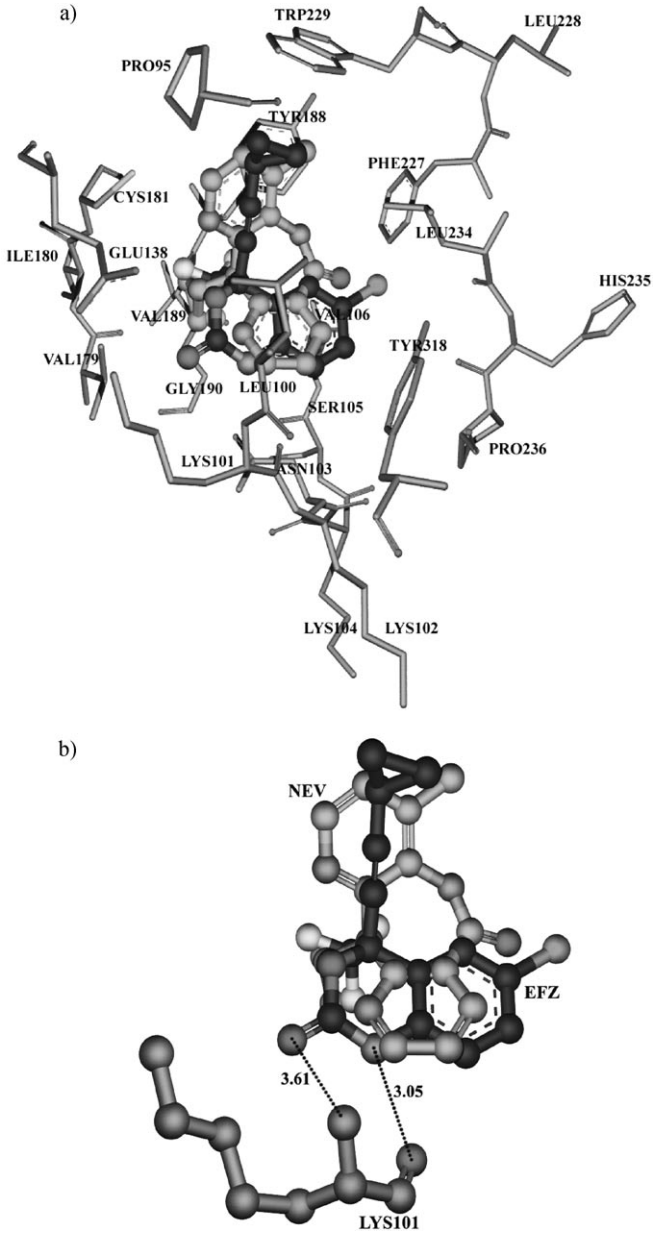

Figure 6. a) Superposition between efavirenz (dark, ball-and-stick) and nevirapine (light, ball-and-stick) in the binding pocket of K103N/Y181C HIV-1 RT. b) Hydrogen bonding interactions between the K101 residue and efavirenz.

Comparing the binding of efavirenz and TMC125, this compound, developed as a potent next generation NNRTIs, can inhibit wild-type, the common single mutants, and double mutants such as K103N/Y181C and K101E/K103N. Its activity against wild-type HIV-1 RT was comparable to the inhibition of efavirenz, however, in the case of mutations, TMC125 shows more activity than nevirapine and efavirenz.[25] The main reason that it can bind to HIV-1 RT enzymes is its multiple conformations of binding which can adapt to side chain changes in the mutations. It can adapt its structure to be the best suitable orientation in the binding pocket of HIV-1 RT. TMC125 has the internal conformational flexibility to produce interactions with the protein binding pocket. Significantly, in molecular details, a hydrogen bonding was found between TMC125 and K101 (Figure 7 b) as is found in the case of efavirenz. In addition, amino hydrogen of benzoxine-2-one and benzene ring of efavirenz are rearranged in the same position with amino linkages of the cyanophenyl substituents of TMC125. However, benzoxine-2-one and benzene ring of efavirenz are rigid, but the ether and amino linkages of the two cyanophenyl substituents of TMC125 provide sufficient flexibility to allow favorable aryl–aryl interactions with Tyr181, Tyr188, Trp229, and Tyr318.[26] These result indicated that TMC125 can be more effective than efavirenz. The most important features are the structural flexibility of NNRTIs[27] and the main interaction be-

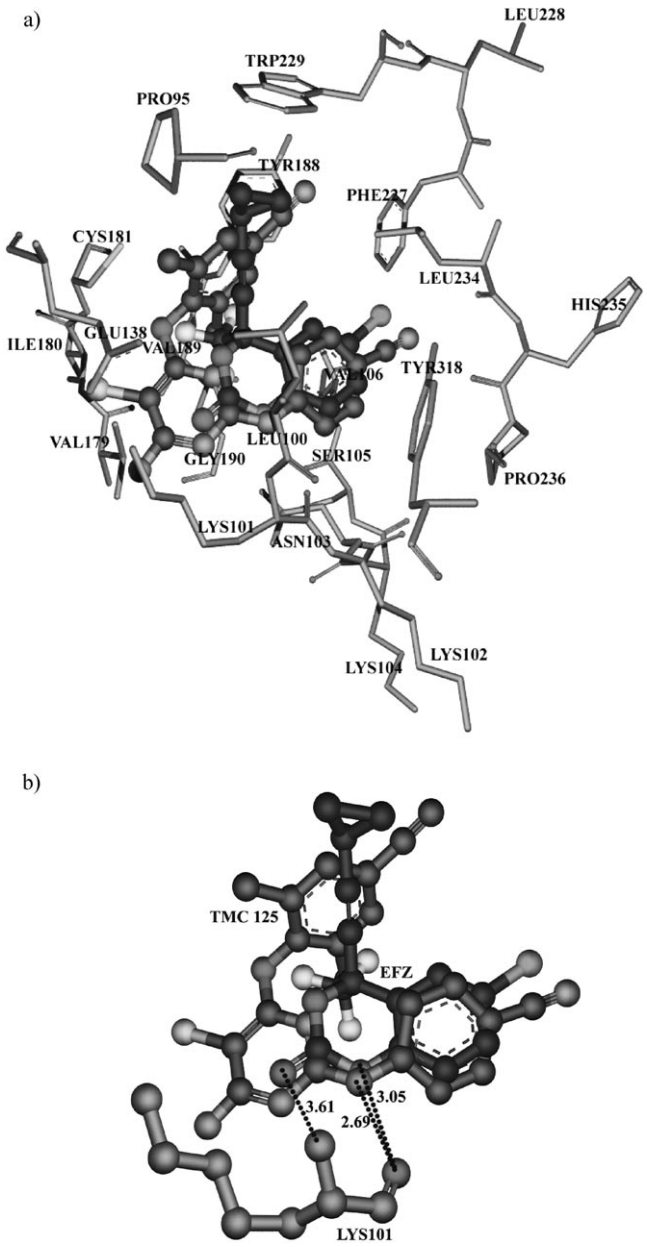

Figure 7. a) Superposition between efavirenz (dark, ball-and-stick) and TMC125 (light, ball-and-stick) in the binding pocket of K103N/Y181C HIV-1 RT. b) Hydrogen bonding interactions between the K101 residue, TMC125, and efavirenz.

tween inhibitor and amino acids surrounding the binding pocket of HIV-1 RT. Therefore, the study of structure-based drug design at the molecular level using quantum chemical calculations can predict interaction of residues in the binding pocket, leading to the design of new potent inhibitors for mutant HIV-1 RTs.

Conclusions

The multilayered integration (ONIOM) method has been applied to determine the different binding energies of efavirenz to K103N/Y181C HIV-1 RT as compared with the wild-type enzyme. The results indicate that the two mutations, K103N and Y181C, eliminate favorable contacts of efavirenz with the aromatic ring of the Y181 and hydrocarbon side chain of K103, leading to a decrease in the stabilizing energy of the complex. Consequently, this leads to more repulsive interactions between efavirenz and the residues of the binding pocket of the K103N/Y181C enzyme relative to the wild-type. By using the ONIOM3 (MP2/6-31G(d,p):B3LYP/6-31G(d,p):PM3) method, the different binding energy can be estimated to be less than that of the wild-type complex, by about 7.91 kcal mol^{-1}. It is important to note that hydrogen bonding occurring between efavirenz and K101 was also disturbed. Moreover, N103 in the binding pocket of the K103N/Y181C enzyme creates a repulsive interaction with the inhibitor. This is consistent with the observation that efavirenz shows a ninefold reduction in inhibitory affinity against K103N/Y181C relative to wild-type HIV-1 RT. Understanding the interactions involved in binding within the pocket, and the structural changes that occur, can be useful for the design of higher potency inhibitors specific to the double mutant enzyme target.

Acknowledgments

The authors thank Prof. Dr. Peter Wolschann and Dr. Mayuso Kuno for valuable critical comments and suggestions. This work was supported with grants from the Thailand Research Fund (RTA5080005). The Commission on Higher Education, Ministry of Education, and Thesis-In-Aid from the Graduate School, Kasetsart University, are acknowledged for partial financial support. The National Excellence Center for Petroleum, Petrochemicals and Advanced Materials, the Large-Scale Simulations Research Laboratory at NECTEC, the National Nanotechnology Center (NANOTEC), Ministry of Science and Technology, Thailand, through its program of Center of Excellence Network, and the ZID of the University of Vienna are appreciated for the use of computing and research facilities. Thanks to Wilhelm J. Holzschuh and Ben Parslew for proofreading this manuscript.

Keywords: binding energy · HIV-1 RT · inhibitor–enzyme interactions · NNRTIs · ONIOM

[1] A. Jacobo-Molina, E. Arnold, *Biochemistry* **1991**, *30*, 6351–6361.
[2] a) E. De Clercq, *Farmaco* **1999**, *54*, 26–45; b) E. De Clercq, *J. Clin. Virol.* **2004**, *30*, 115–133; c) S. G. Sarafianos, S. H. Hughes, E. Arnold, *Int. J. Biochem. Cell Biol.* **2004**, *36*, 1706–1715; d) G. Campiani, A. Ramunno, G. Maga, V. Nacci, C. Fattorusso, B. Catalanotti, E. Morelli, E. Novellino, *Curr. Pharm. Des.* **2002**, *8*, 615–657; e) P. G. Wyatt, R. C. Bethell, N. Cammack, D. Charon, N. Dodic, B. Dumaitre, D. N. Evans, D. V. S. Green, P. L. Hopewell, D. C. Humber, R. B. Lamont, D. C. Orr, S. J. Plested, D. M. Ryan, S. L. Sollis, R. Storer, G. G. Weingartent, *J. Med. Chem.* **1995**, *38*, 1657–1665.
[3] a) J. Wang, P. Morin, W. Wang, P. A. Kollman, *J. Am. Chem. Soc.* **2001**, *123*, 5221–5230; b) J. Ren, R. Esnouf, E. German, D. Somers, C. Ross, I. Kirby, J. Keeling, G. Darby, Y. Jones, D. I. Stuart, D. K. Stammers, *Nat. Struct. Biol.* **1995**, *2*, 293–302.
[4] a) R. F. Schinazi, B. A. Larder, J. W. Mellors, *International Antiviral News* **1997**, *5*, 129–135; b) C. Mao, E. A. Sudbeck, T. K. Venkatachalam, F. M. Uckun, *Biochem. Pharmacol.* **2000**, *60(9)*, 1251–1265; c) J. D. Pata, W. G. Stirtan, S. W. Goldstein, T. A. Steitz, *Proc. Natl. Acad. Sci. USA* **2004**, *101(29)*, 10548–10553; d) Y. Hsiou, J. Ding, K. Das, A. D. Clark, J. P. Kleim, M. Rosner, I. Winkler, G. Riess, S. H. Hughes, E. Arnold, *J. Mol. Biol.* **1998**,

284, 313–323; e) Y. Hsiou, J. Ding, K. Das, A. D. Clark, P. L. Boyer, P. Lewi, P. A. J. Janssen, M. Rosner, S. H. Hughes, E. Arnold, *J. Mol. Biol.* **2001**, *309*, 437–445.

[5] a) J. Ren, J. Milton, K. L. Weaver, S. A. Short, D. I. Stuart, D. K. Stammers, *Structure* **2000**, *8*, 1089–1094; b) J. Lindberg, S. Sigurosson, S. Lowgren, H. O. Andersson, C. Sahlberg, R. Noreen, K. Fridborg, H. Zhang, T. Unge, *Eur. J. Biochem.* **2002**, *269*, 1670–1677; c) J. Ren, C. Nichols, L. Bird, P. Chamberlain, D. I. Stuart, D. K. Stammers, *J. Mol. Biol.* **2001**, *312*, 795–805.

[6] S. D. Young, S. F. Britcher, L. E. Tran, L. S. Payne, W. C. Lumma, T. A. Lyle, J. R. Huff, P. S. Anderson, D. B. Olsen, S. S. Carroll, D. J. Pettibone, J. A. O'Brien, R. G. Ball, S. K. Balani, J. H. Lin, I. W. Chen, W. A. Schleif, V. V. Sardana, W. J. Long, V. W. Byrnes, E. A. Emini, *Antimicrob. Agents Chemother.* **1995**, *39*, 2602–2605.

[7] M. Udier-Blagovic, E. K. Watkins, J. Tirado-Rives, W. L. Jorgensen, *Bioorg. Med. Chem. Lett.* **2003**, *13*, 3337–3340.

[8] M. Udier-Blagovic, J. Tirado-Rives, W. L. Jorgensen, *J. Med. Chem.* **2004**, *47*, 2389–2392.

[9] F. Rodriguez-Barrios, J. Balzarini, F. Gago, *J. Am. Chem. Soc.* **2005**, *127*, 7570–7578.

[10] P. Weinzinger, S. Hannongbua, P. Wolschann, *J. Enzyme Inhib. Med. Chem.* **2005**, *20*, 129–134.

[11] P. Pungpo, P. Saparpakorn, P. Wolschann, S. Hannongbua, *SAR QSAR Environ. Res.* **2006**, *17*, 353–370.

[12] a) L. Ridder, A. J. Mulholland, *Curr. Top. Med. Chem.* **2003**, *3*, 1241–1256; b) A. J. Mulholland, *Drug discovery today* **2005**, *10*, 1393–1402; c) A. Warshel, M. Levitt, *J. Mol. Biol.* **1976**, *103*, 227–249.

[13] Y. Mei, X. He, Y. Xiang, D. W. Zhang, J. Z. H. Zhang, *Proteins Struct. Funct. Genet.* **2005**, *59*, 489–495.

[14] K. Morokuma, *Philos. Transact. A Math. Phys. Eng. Sci.* **2002**, *360*, 1149–1164.

[15] a) M. Svensson, S. Humbel, R. D. J. Froese, T. Matsubara, S. Sieber, K. Morokuma, *J. Phys. Chem.* **1996**, *100*, 19357–19363; b) S. Dapprich, I. Komaromi, K. S. Byun, K. Morokuma, M. J. Frisch, *J. Mol. Struct. (Theochem)* **1999**, *1–21*, 461–462; c) K. Morokuma, *Bull. Korean Chem. Soc.* **2003**, *24*, 797–801; d) T. Vreven, K. S. Byun, I. Komaromi, S. Dapprich, J. A. Montgomery, K. Morokuma, M. J. Frisch, *J. Chem. Theory Comput.* **2006**, *2*, 815–826; e) K. Morokuma, O. Wang, T. Vreven, *J. Chem. Theory Comput.* **2006**, *2*, 1317–1324.

[16] a) S. Saen-oon, M. Kuno, S. Hannongbua, *Proteins Struct. Funct. Genet.* **2005**, *61*, 859–869; b) M. Kuno, S. Hannongbua, K. Morokuma, *Chem. Phys. Lett.* **2003**, *380*, 456–463.

[17] P. Nunrium, M. Kuno, S. Saen-oon, S. Hannongbua, *Chem. Phys. Lett.* **2005**, *405*, 198–202.

[18] M. J. Frisch, G. W. Trucks, H. B. Schlegel, G. E. Scuseria, M. A. Robb, J. R. Cheeseman, J. A. Montgomery, Jr., T. Vreven, K. N. Kudin, J. C. Burant, J. M. Millam, S. S. Iyengar, J. Tomasi, V. Barone, B. Mennucci, M. Cossi, G. Scalmani, N. Rega, G. A. Petersson, H. Nakatsuji, M. Hada, M. Ehara, K. Toyota, R. Fukuda, J. Hasegawa, M. Ishida, T. Nakajima, Y. Honda, O. Kitao, H. Nakai, M. Klene, X. Li, J. E. Knox, H. P. Hratchian, J. B. Cross, C. Adamo, J. Jaramillo, R. Gomperts, R. E. Stratmann, O. Yazyev, A. J. Austin, R. Cammi, C. Pomelli, J. W. Ochterski, P. Y. Ayala, K. Morokuma, G. A. Voth, P. Salvador, J. J. Dannenberg, V. G. Zakrzewski, S. Dapprich, A. D. Daniels, M. C. Strain, O. Farkas, D. K. Malick, A. D. Rabuck, K. Raghavachari, J. B. Foresman, J. V. Ortiz, Q. Cui, A. G. Baboul, S. Clifford, J. Cioslowski, B. B. Stefanov, G. Liu, A. Liashenko, P. Piskorz, I. Komaromi, R. L. Martin, D. J. Fox, T. Keith, M. A. Al-Laham, C. Y. Peng, A. Nanayakkara, M. Challacombe, P. M. W. Gill, B. Johnson, W. Chen, M. W. Wong, C. Gonzalez, J. A. Pople, *Gaussian 03*, revision B.05;Gaussian, Inc.: Pittsburgh, **2003**.

[19] a) S. Kristyán, P. Pulay, *Chem. Phys. Lett.* **1994**, *229*, 175–180; b) S. Tsuzuki, H. P. Luthi, *J. Chem. Phys.* **2001**, *114*, 3949.

[20] a) S. F. Boys, F. Bernardi, *Mol. Phys.* **1970**, *19*, 553–566; b) M. Kuno, R. Hongkrengkai, S. Hannongbua, *Chem. Phys. Lett.* **2006**, *424*, 172–177.

[21] K. Das, S. G. Sarafianos, A. D. Clark, P. L. Boyer, S. H. Hughes, E. Arnold, *J. Mol. Biol.* **2007**, *365*, 77–89.

[22] P. A. Janssen, P. J. Lewi, E. Arnold, F. Daeyaert, M. de Jonge, J. Heeres, *J. Med. Chem.* **2005**, *48*, 1901–1909.

[23] G. M. Morris, D. S. Goodsell, A. J. Olson, The Scripps Research Institute, AutoDock 3.05, **2000**.

[24] Y. Hsiou, J. Ding, K. Das, A. D. Clark, P. L Boyer, et al., *J. Mol. Biol.* **2001**, *309*, 437–445.

[25] K. Andries, H. Azijn, T. Thielemans, D. Ludovici, M. Kukla, J. Heeres, P. Janssen, B. D. Corte, J. Vingerhoets, R. Pauwels, M. P. de Béthune, *Antimicrob. Agents Chemother.* **2004**, *48*, 4680–4686.

[26] K. Das, A. D. Clark, P. J. Lewi, J. Heeres, M. R. de Jonge, L. M. H. Koymans, H. M. Vinkers, F. Daeyaert, D. W. Ludovici, M. J. Kukla, B. D. Corte, R. W. Kavash, C. Y. Ho, H. Ye, M. A. Lichtenstein, K. Andries, R. Pauwels, P. L. Boyer, P. Clark, S. H. Hughes, P. A. J. Janssen, and E. Arnold, *J. Med. Chem.* **2004**, *47*, 2550–2560.

[27] a) L. Lawtrakul, S. Hannongbua, A. Beyer, P. Wolschann, *Biol. Chem.* **1999**, *380*, 265–267; b) L. Lawtrakul, S. Hannongbua, A. Beyer, P. Wolschann, *Monatsh. Chem.* **1999**, *130*, 1347–1363; c) S. Hannongbua, S. Saen-oon, P. Pungpo, P. Wolschann, *Monatsh. Chem.* **2001**, *132*, 1157–1169; d) S. Hannongbua, S. Prasithichokekul, P. Pungpo, *J. Comput.-Aided Mol. Des.* **2001**, *15*, 997–1004.

Received: July 26, 2007
Revised: December 21, 2007
Published online on March 12, 2008

